

RESEARCH ARTICLE

Mitochondrial dysfunction in iPSC-derived neurons of subjects with chronic mountain sickness

Helen Zhao,¹ Guy Perkins,² Hang Yao,¹ David Callacondo,^{7,8} Otto Appenzeller,⁹ Mark Ellisman,² Albert R. La Spada,^{1,3,4,5,6,10} and Gabriel G. Haddad^{1,3,10}

¹Department of Pediatrics (Respiratory Medicine), University of California San Diego, La Jolla, California; ²National Center for Microscopy and Imaging Research, University of California San Diego, La Jolla, California; ³Department of Neurosciences, University of California San Diego, La Jolla, California; ⁴Department of Cellular and Molecular Medicine, University of California San Diego, La Jolla, California; ⁵Institute for Genomic Medicine, University of California San Diego, La Jolla, California; ⁶Sanford Consortium for Regenerative Medicine, University of California San Diego, La Jolla, California; ⁷School of Medicine, Faculty of Health Sciences, Universidad Privada de Tacna, Tacna, Peru; ⁸Instituto de Evaluación de Tecnologías en Salud e Investigación (IETSI), EsSalud, Lima, Peru; ⁹New Mexico Health Enhancement and Marathon Clinics Research Foundation, Albuquerque, New Mexico; and ¹⁰The Rady Children's Hospital, San Diego, California

Submitted 26 July 2017; accepted in final form 12 December 2017

Zhao H, Perkins G, Yao H, Callacondo D, Appenzeller O, Ellisman M, La Spada AR, Haddad GG. Mitochondrial dysfunction in iPSC-derived neurons of subjects with chronic mountain sickness. *J Appl Physiol* 125: 832–840, 2018. First published December 21, 2017; doi:10.1152/jappphysiol.00689.2017.—Patients with chronic mountain sickness (CMS) suffer from hypoxemia, erythrocytosis, and numerous neurologic deficits. Here we used induced pluripotent stem cell (iPSC)-derived neurons from both CMS and non-CMS subjects to study CMS neuropathology. Using transmission electron microscopy, we report that CMS neurons have a decreased mitochondrial volume density, length, and less cristae membrane surface area. Real-time PCR confirmed a decreased mitochondrial fusion gene optic atrophy 1 (OPA1) expression. Immunoblot analysis showed an accumulation of the short isoform of OPA1 (S-OPA1) in CMS neurons, which have reduced ATP levels under normoxia and increased lactate dehydrogenase (LDH) release and caspase 3 activation after hypoxia. Improving the balance between the long isoform of OPA1 and S-OPA1 in CMS neurons increased the ATP levels and attenuated LDH release under hypoxia. Our data provide initial evidence for altered mitochondrial morphology and function in CMS neurons, and reveal increased cell death under hypoxia due in part to altered mitochondrial dynamics.

NEW & NOTEWORTHY Induced pluripotent stem cell-derived neurons from chronic mountain sickness (CMS) subjects have altered mitochondrial morphology and dynamics, and increased sensitivity to hypoxic stress. Modification of OPA1 can attenuate cell death after hypoxic treatment, providing evidence that altered mitochondrial dynamics play an important role in increased vulnerability under stress in CMS neurons.

chronic mountain sickness; mitochondrial dysfunction; neuron; OPA1

INTRODUCTION

Chronic mountain sickness (CMS) is a disease that threatens a large segment of the high-altitude population (more than 140

million highlanders) during extended living at altitudes of over 2,500 m. Patients with CMS suffer from severe hypoxemia, excessive erythrocytosis, and neurologic manifestations including migraine, mental fatigue, confusion, and memory loss. In Andeans, the prevalence of CMS is about 15–20%; the majority of highlanders (non-CMS) keep physically healthy and well adapted at high altitude (27). Therefore CMS is believed to be a maladaptation to hypoxia.

Mitochondria have been shown to play an important role in hypoxia tolerance or adaptation in mammals, including rats, *Drosophila*, and humans (13, 21, 29). For instance, mitochondrial haplogroups G and M9a1a1c1b, with especially the T3394C (ND1) and G7697A (COXII) variants, are believed to be the cause of hypoxic adaptation in Tibetans (21). Therefore we hypothesize that mitochondrial genetic modification may be involved in hypoxia adaptation in Andeans, with mitochondrial differences between non-CMS and CMS accounting for the clinical differences observed between the two groups.

Mitochondria are not only key organelles for energy production but also play an important role in aging and aging-related diseases such as diabetes, cancer, Alzheimer's disease and Parkinson's disease (15, 23, 31). As dynamic organelles, mitochondria undergo constant fission and fusion, which are an important mechanism for modulating redox status, mitochondrial integrity, function, and cell death signaling pathways (22). Of interest is that mitochondrial fragmentation and dysfunction are an early event in neurodegeneration and likely contribute to the progressive loss of neurons in patients with Alzheimer's or Parkinson's disease (31, 45). CMS subjects have a number of neurological signs and symptoms, including migraine, mental fatigue, confusion, and memory loss in central nervous system, as well as mild demyelination on pathologic examination of the peripheral nervous system (41). However, due to the lack of *ex vivo* samples and techniques, our understanding of CMS neuropathology is still very limited. Induced pluripotent stem cell (iPSC) technology enables us to investigate the morphology and function of iPSC-derived CMS neurons. We report that CMS neurons exhibit altered mitochondrial morphology and

Address for reprint requests and other correspondence: G. G. Haddad, Dept. of Pediatrics and Neuroscience, Univ. of California San Diego, 9500 Gilman Dr., La Jolla, CA 92093-0735 (e-mail: ghaddad@ucsd.edu).

mitochondrial dynamics, accompanied by increased mitochondrial fragmentation and disrupted ATP levels. In addition, CMS neurons have increased lactate dehydrogenase (LDH) release and caspase 3 activation after hypoxic treatment, and this susceptibility to hypoxic stress can be attenuated through the manipulation of OPA1, which promotes mitochondrial fusion.

MATERIALS AND METHODS

Neuronal culture. All subjects in the present study were adult native men residing in the Andean mountain range their entire life, in Cerro de Pasco, Peru, at an elevation of ~4,338 m. CMS patients fulfilled the diagnostic criteria for CMS based on their hematocrit, O₂ saturation, and CMS score (>12) (43). Those with CMS score <5 were chosen as non-CMS subjects (Table 1). Each subject signed an informed, written consent form under protocols approved by the University of California San Diego and the Universidad Peruana Cayetano Heredia. As described before, skin biopsies from non-CMS (n = 4) and CMS (n = 5) subjects were collected in Peru. Fibroblasts from the skin biopsies were cultured and were reprogrammed into iPSCs in San Diego. iPSC-derived NPCs were generated following an embryoid body formation protocol. Neural differentiation was initiated by withdrawing FGF2 when cells reached 70% confluence (48).

Transmission electron microscopy. Neurons were fixed using 2.5% glutaraldehyde and 2% paraformaldehyde in 0.1 M sodium cacodylate, pH 7.4, for 1 h on ice. The fixed cells were then washed three times with ice-cold 0.1 M sodium cacodylate for 5 min on ice followed by postfixation in 1% osmium tetroxide and 0.8% potassium ferrocyanide in 0.1 M sodium cacodylate for 2 h on ice. After three washes in ice-cold ddH₂O for 5 min each, the cells were stained in 2% uranyl acetate for 1 h. Samples were dehydrated in an ethanol series of ice-cold 20, 50, 70, 90% then three washes in 100% ethanol at room temperature (RT) for 5 min each. Samples were infiltrated in 50% ethanol-50% Durcupan ACM for 3 h at RT with agitation, followed by three changes of 100% Durcupan for 8 h each at RT with agitation. The Durcupan resin was polymerized at 60°C for 2 days under vacuum. Sectioning was performed using a Leica ultramicrotome. Sections were cut at a nominal thickness of 70 nm and were post-stained with uranyl acetate (5 min) and lead salts (2 min) before imaging using an FEI Spirit transmission electron microscope (EM) operated at 120 kV. Sampling bias was avoided by first selecting the area of the culture dish randomly from which the sections were cut. The EM images were taken strictly randomly. The images were collected with a charge-coupled device digital camera with 2 × 2 k pixels at a magnification of ×4,400 corresponding to a pixel resolution of 2.9 nm. Each electron micrograph covered an area of 6 by 6 μm, and each section appeared to slice through several neurons each with a number of dendrites. The density of neurons was similar across subjects, including non-CMS and CMS.

Mitochondrial volume density (volume fraction), cristae abundance, and length were measured on the EM images. The mitochondrial volume density, defined as the volume occupied by mitochondria divided by the volume occupied by the cytoplasm, was measured using stereology with the aid of Adobe Photoshop. Point counting was used to determine the mitochondrial volume densities by overlaying a grid on each digitized image. Mitochondria and cytoplasm lying under intercepts were counted. The relative volume of mitochondria was expressed as the ratio of intercepts coinciding with this organelle to the intercepts coinciding with cytoplasm and reported as a percentage. Mitochondrial cristae abundance is defined as the sum of the cristae membrane surface divided by the outer membrane surface area with the aid of the ImageJ free-hand tool. Mitochondrial lengths were measured on these same images by using the ImageJ line segment tool.

Table 1. Summary of non-CMS and CMS subjects from Cerro de Pasco used in the present study as well as their medical test scores

Group	Subject ID	Age	Dizziness	Physical Weakness	Mental Fatigue	Anorexia	Muscle Weakness	Joint Pain	Breathlessness	Palpitations	Disturbed Sleep	Cyanosis	Injected Conjunctive	Dilation	Paresthesia	Headache	Tinnitus	Hct Score	Sat Score	CMS Score
Non-CMS	1	33	1	0	0	0	0	0	0	0	2	2	0	2	0	0	0	0	0	7
	2	31	0	0	0	0	0	0	0	0	0	0	0	0	0	0	0	0	0	0
	3	23	0	0	0	0	0	0	0	0	0	0	0	0	0	3	0	0	0	3
	4	31	0	0	0	0	0	0	0	0	0	0	0	0	0	0	0	0	0	0
CMS	1	22	0	0	0	0	0	0	2	2	2	2	2	0	2	3	3	3	0	21
	2	37	0	0	0	1	0	1	2	0	0	2	2	0	2	3	0	3	3	19
	3	34	0	0	1	0	1	0	0	0	2	2	0	0	2	3	3	3	0	17
	4	34	0	1	1	0	0	1	2	2	0	2	2	0	0	3	0	3	3	22
	5	43	0	1	1	0	0	1	2	2	2	2	2	2	0	3	3	3	3	27

CMS, chronic mountain sickness; Hct, hematocrit; Sat, O₂ saturation.

Real-time PCR. Total RNA was extracted using the RNase Mini kit (Qiagen, CA). After removing genomic DNA with DNase I digestion (Ambion, TX), 500 ng of total RNA was converted to complementary of DNA by using SuperScript First-Strand Synthesis System for RT-PCR (Life Technologies, CA). Quantification was performed using an Applied Biosystems 7500 Real Time Sequence Detection System with Power SYBR Green qPCR Master Mix (Life Technologies, CA) and actin as a loading control.

Western blot analysis. Neurons were homogenized in RIPA buffer plus protease and phosphatase inhibitors (1 mM phenylmethylsulfonyl fluoride and 1 × protease inhibitor cocktail). Homogenates were then centrifuged for 10 min at 10,000 *g* and 4°C. The supernatants were collected and protein concentration was determined using a Bio-Rad protein assay kit (Bio-Rad, CA). Fifteen micrograms of protein was separated following the standard protocol with anti-OPA1 (1:1,000; BD Bioscience) or anti-Casp3 (1:500; Biologend, CA); immunoreactive bands were visualized using Bio-Rad ChemiDoc XRS with enhanced chemiluminescence (PerkinElmer, MA). Equal loading was assessed using anti-actin (1:1,000; Santa Cruz Biotechnology, CA), and data were analyzed using ImageLab software (version 3.0, Bio-Rad).

ATP assay. Intracellular ATP level was determined by ATPlite assay (PerkinElmer), following the manufacturer's protocol. The production of luminescence light caused by the reaction of ATP with added luciferase, and D-luciferin was proportional to the intracellular ATP level. In brief, the same number of cells (1×10^5) was collected and lysed. After adding substrate, the luminescence signal was measured by Wallac Victor2 1420 multilabel counter (PerkinElmer). ATP data were presented as percentage changes relative to non-CMS or CMS as indicated.

LDH cytotoxicity assay. Neurons were treated with 1 or 1.5% O₂ for 2 to 4 days, and LDH release from the cells was determined in the cell-free culture supernatant by using a LDH cytotoxicity detection kit according to the manufacturer's protocols (Clontech). The percentage of LDH vs. the maximal LDH in each sample was compared.

Fluorescence imaging of mitochondria. To image the mitochondrial morphology in both CMS and non-CMS neurons, Neurons that

were cultured on the coverslip were loaded with 1 μM of MitoTracker Green FM (Invitrogen, CA) for 1 h in the incubator and then mounted with antifade reagent for imaging. Mitochondrial imaging was performed to examine the fragmentation of mitochondria by using a two-photon confocal laser scanning microscope (Olympus Fluoview 1000, Olympus). Each sample was scanned with a ×63 Plan-Neofluar oil objective with a high numerical aperture (1.4) lens at 1,600 × 1,600 pixel resolution. Mitochondrial particles with strong labeling (compared with background) and clear edges confined in soma were used to measure the mitochondrial length. All measurements were performed using ImageJ. Approximately ~450 mitochondria were measured each group.

Lentivirus transfection. The pMSCV-OPA1 construct was a generous gift from Dr. David Chen's laboratory (University of Southern California, Los Angeles, CA). The packaging and retrovirus generation was done by Burnham Institute Gene Transfer, Targeting and Therapeutics Core (La Jolla, CA). After transfection, iPSCs were selected with 1 μg/ml of puromycin (Sigma). The OPA1 expression was confirmed by immunoblot.

Statistics. All experiments were repeated at least twice, and data were collected from four to five individuals in each group. Results were expressed as group means ± SE, and data were graphed using GraphPad Prism 4.02 (GraphPad Software, CA). Differences were considered statistically significant when $P < 0.05$, using both parametric (*t*-tests) and nonparametric (Wilcoxon rank sum test) statistics.

RESULTS

Altered mitochondrial structure in CMS neurons. To test the hypothesis that mitochondrial modifications contribute to hypoxia adaptation in non-CMS subjects, we examined the structure of mitochondria in the iPSC-derived neurons by employing transmission electron microscopy. Figure 1A shows an example of a typical non-CMS mitochondrion (*top*) and smaller, clustered CMS mitochondria (*bottom*). A significantly decreased mitochondrial volume density (Fig. 1B, $P = 0.02$),

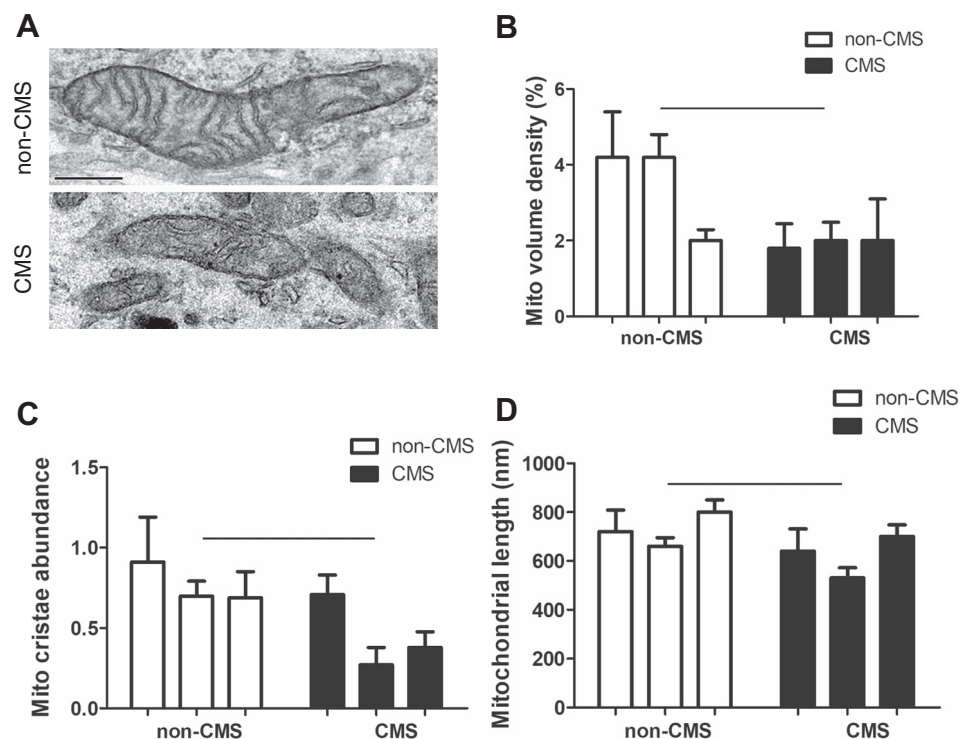


Fig. 1. Altered mitochondrial structure in chronic mountain sickness (CMS) neurons. A: representative transmission electron microscopy images of mitochondria from non-CMS and CMS. B: a decreased mitochondrial (Mito) volume density in CMS neurons. C: a decreased mitochondrial cristae area in CMS neurons. D: a decreased mitochondrial length in CMS neurons. The scale bar is 250 nm; $n = 3$, $P < 0.05$.

cristae abundance (Fig. 1C, $P = 0.02$), and shorter mitochondria (Fig. 1D, $P = 0.03$) were observed in CMS neurons, indicating fewer and smaller mitochondria in CMS neurons.

Altered mitochondrial dynamics in CMS neurons. Homeostasis of mitochondrial mass is maintained by the balance between biogenesis and mitophagy, which are tightly coordinated and reciprocally interacting processes. Peroxisome proliferator-activated receptor- γ (PPAR γ) coactivator-1 α (PGC-1 α) is a master regulator of mitochondrial biogenesis, whereas PARK2 is mainly responsible for mitophagy. Using real-time PCR, we found a significantly decreased PGC-1 α mRNA expression and significantly increased PARK2 mRNA expression in CMS neurons compared with non-CMS neurons (Fig. 2A, $P = 0.03$), suggesting an imbalance in mitochondrial mass homeostasis due to decreased mitochondrial biogenesis and increased mitophagy.

Dynamic regulation of mitochondria through fission and fusion is an important mechanism for modulation of redox status, mitochondria integrity, function, and cell death signaling pathways (22). Both fission genes DRP1 and FIS1 and fusion genes optic atrophy 1 (OPA1) and MFN2 were significantly underexpressed in CMS neurons (Fig. 2B, $P = 0.04$). OPA1 is a dynamin-related guanosine triphosphatase protein and plays a critical role in regulating mitochondrial innermembrane fusion and cristae structure. In mitochondria, the N-terminal mitochondrial targeting sequence of the OPA1 precursor is cleaved to the OPA1 long isoform (L-OPA1), which is further cleaved to the short isoform of OPA1 (S-OPA1). L-OPA1 promotes fusion and S-OPA1 promotes fission (35). Using Western blot analysis, we found that S-OPA1 accumulate significantly in CMS neurons compared with non-CMS neurons, evidenced by increased S-OPA1 expression relative

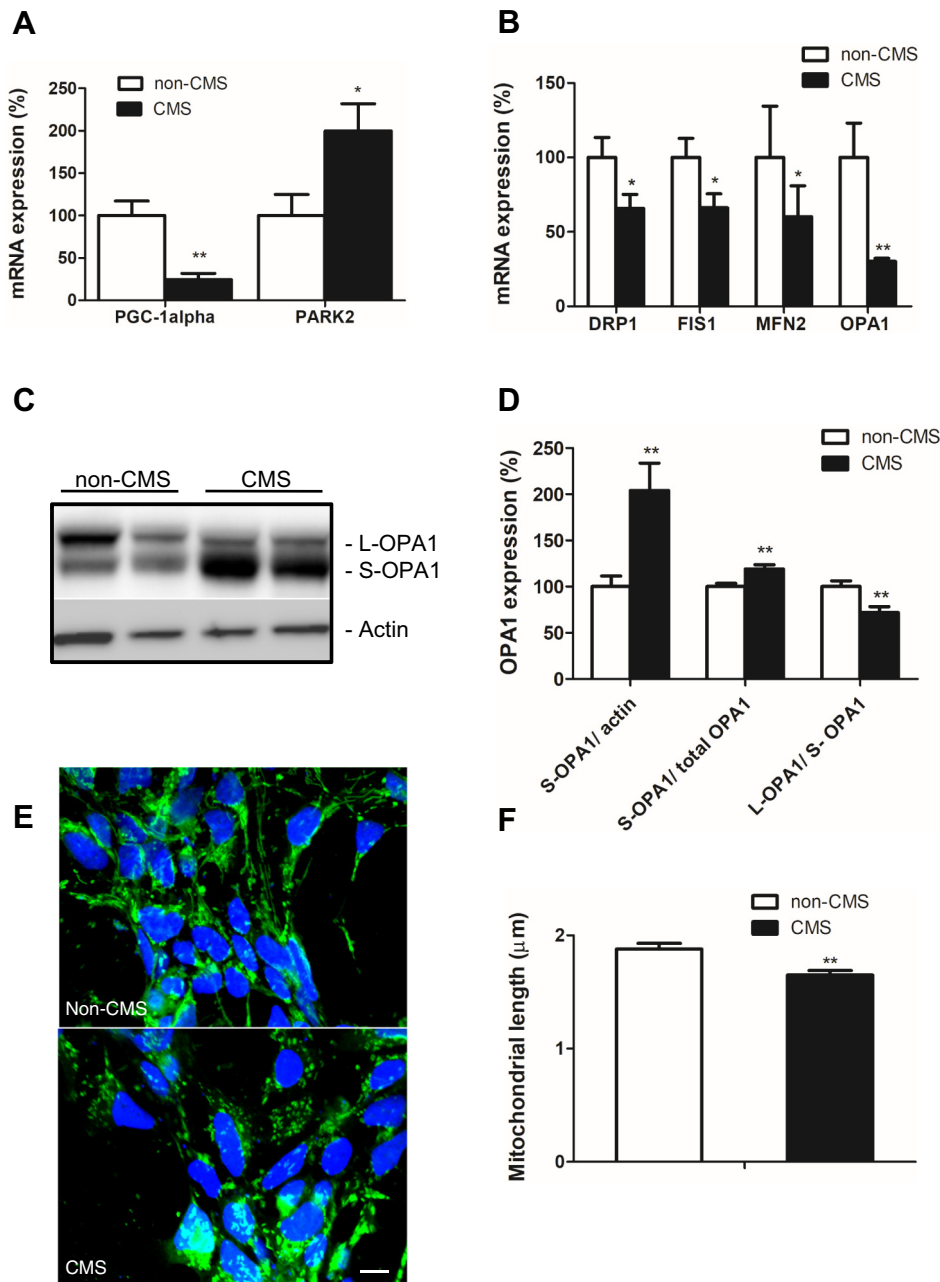


Fig. 2. Altered mitochondrial gene and protein expression in CMS neurons. *A*: mRNA gene expression profiles of mitochondrial biogenesis gene PGC-1 α and mitophagy gene PARK2. *B*: mRNA gene expression profiles of mitochondrial fission genes (FIS1 and DRP1) and fusion genes (OPA1 and MFN2). *C*: a representative blot of OPA1 in non-CMS and CMS neurons. *D*: quantification of OPA1 between the two groups; $n = 3$. *E*: a representative image of mitochondria labeled with MitoTracker Green FM in non-CMS and CMS neurons. *F*: quantification of mitochondrial length between non-CMS ($n = 4$) and CMS ($n = 5$). The scale bar is 10 μ m; * $P < 0.05$, ** $P < 0.01$.

to actin and total OPA1 as well as a decreased L-OPA1/S-OPA1 ratio (Fig. 2, *C* and *D*, $P = 0.007$), suggesting more fission, fragmented and shorter mitochondria in these cells. Shorter mitochondria were also observed by immunostaining with fluorescence marker MitoTracker Green FM (Fig. 2, *E* and *F*, $P = 0.003$).

Altered mitochondrial function in CMS neurons. Previous studies have shown that mitochondrial fragmentation can lead to energy disruption, cytochrome *c* release, caspase activation, and eventually cell death after exposure to ischemia-reperfusion (33, 38). Therefore we speculated that similar changes might occur in CMS neurons. As shown in Fig. 3*A*, we indeed observed a significant decrease in ATP levels in CMS neurons compared with non-CMS neurons, indicating energy disruption in CMS neurons. By exposing neurons to 1% O₂ for 72 h, we found that LDH release was significantly increased in CMS neurons compared with non-CMS neurons (Fig. 3*B*, $P = 0.04$), indicating an increased susceptibility to hypoxic stress in CMS neurons. Since hypoxia treatment is well known to induce caspase pathway-mediated apoptosis (19, 49), we measured expression of cleaved caspase 3 as a marker of caspase 3 activation by immunoblot analysis and observed significantly increased caspase 3 activation in CMS neurons after 2 days of hypoxia treatment (Fig. 3, *C* and 3*D*, $P = 0.02$). Furthermore, increased caspase 3 activation in CMS neurons was correlated with an increased cleavage of L-OPA1 and accumulation of S-OPA1 (Fig. 3*C*).

Modification of OPA1 expression attenuates LDH release in CMS neurons under hypoxia. Previous studies have shown that hypoxic treatment induces S-OPA1 accumulation and caspase 3 overactivation (39); therefore we hypothesize that S-OPA1 accumulation observed in CMS neurons renders cells to commit to caspase 3-mediated cell death and leads to an increased vulnerability under hypoxia. We altered OPA1 gene expression in CMS neurons, exposed these modified CMS neurons

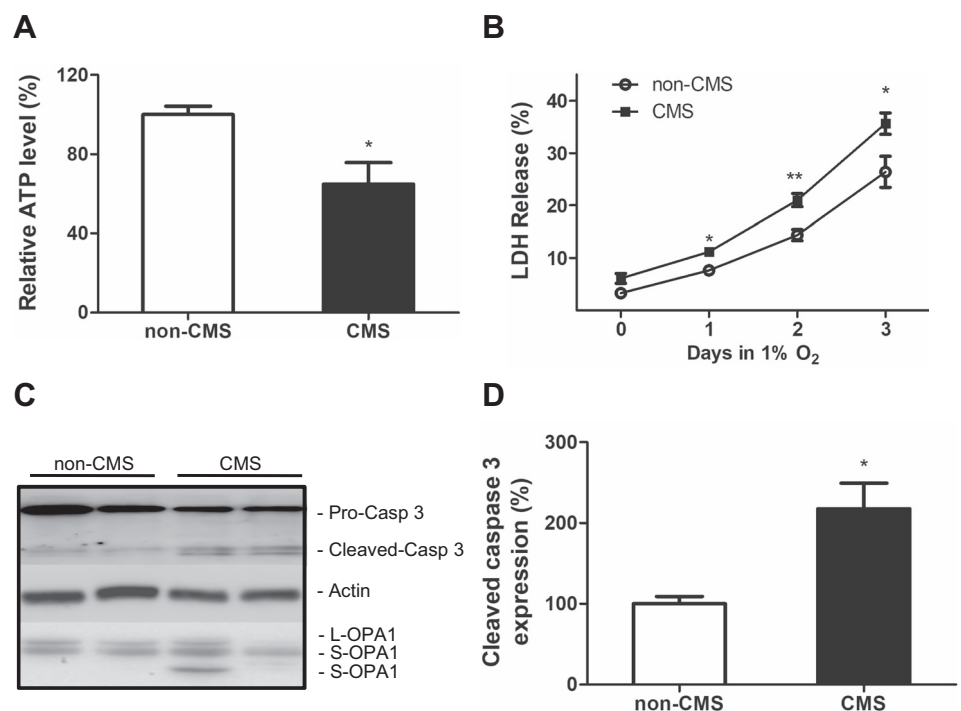
(mCMS-OPA1) to hypoxia, and studied their LDH release. As shown in Fig. 4, *A* and *B*, by transfecting iPSC with OPA1, we were able to increase the amount of L-OPA1 and improve the balance between L- and S-OPA1 (L/S-OPA1 ratio) (Fig. 4, *A* and *B*, $P = 0.03$). These mCMS-OPA1 neurons have an increased ATP level compared with CMS cells alone (Fig. 4*C*, $P = 0.003$), demonstrating an improved balance between L- and S-OPA1 promotes energy maintenance.

In addition, a significantly decreased LDH release was observed in mCMS-OPA1 neurons compared with CMS neurons after 2 and 4 days of 1.5% O₂ treatment (Fig. 4*D*, $P = 0.01$), and a significantly decreased caspase 3 activation was confirmed at *day 2* (Fig. 4, *E* and *F*, $P = 0.04$), demonstrating that modification of OPA1 can delay the initiation of caspase 3-mediated cell death in mCMS-OPA1 neurons. However, modified OPA1 does not restore the survival of mCMS-OPA1 neurons back to the level of non-CMS neurons, as non-CMS neurons still have a significantly lower LDH release than mCMS-OPA1 neurons under 4 days of hypoxia, indicating that modification of OPA1 expression can attenuate LDH release in CMS neurons, but the altered mitochondrial dynamics, due to imbalanced L- and S- isoforms of OPA1, contribute partially to the increased susceptibility in CMS neurons under hypoxia stress.

DISCUSSION

Chronic mountain sickness (CMS) was first described by Carlos Monge in 1925. The disease potentially threatens >140 million highlanders during extended living over 2,500 m. Compared with healthy highlanders, CMS subjects have a number of neuropathological features, including migraine, mental fatigue, confusion, memory loss (43), reduced cerebral blood flow, and delayed cerebral circulation, with the decrease in cerebral blood being correlated with the increasing severity

Fig. 3. Increased susceptibility to hypoxia in CMS neurons. *A*: a decreased ATP level in CMS neurons ($n = 5$) compared with non-CMS neurons ($n = 4$). *B*: an increased LDH release in CMS neurons ($n = 5$) after 3 days of 1% O₂ treatment compared with non-CMS neurons ($n = 4$). *C*: a representative blot of caspase 3 and OPA1 in non-CMS and CMS neurons after 1% O₂ treatment for 2 days. *D*: quantification of cleaved caspase 3 between the two groups; $n = 3$, * $P < 0.05$, ** $P < 0.01$.



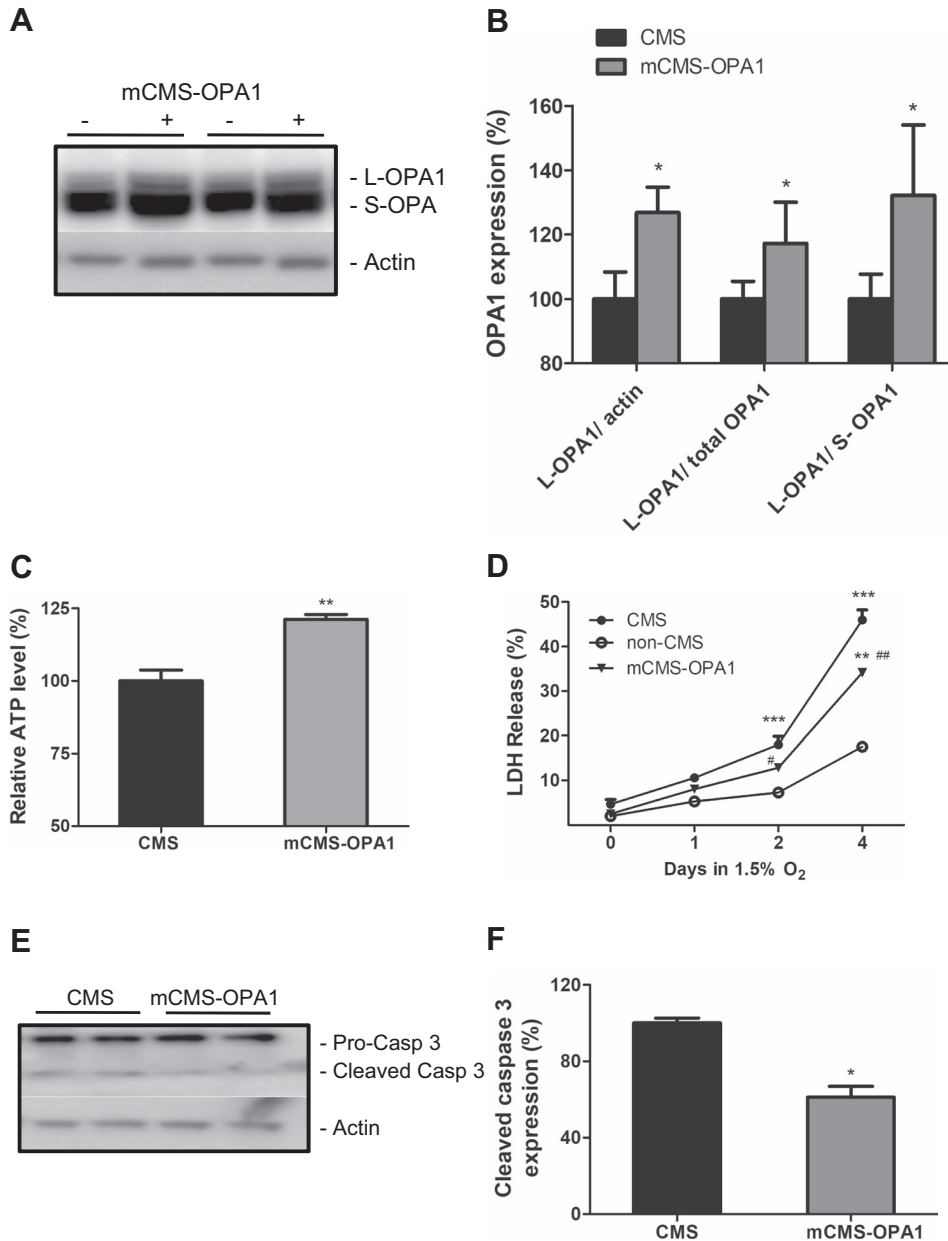


Fig. 4. Improved survival rate after hypoxia treatment by modification of OPA1 expression in CMS neurons. *A*: representative blot of OPA1 expression in CMS and mCMS-OPA1 cells. *B*: quantification of OPA1 between the two groups. *C*: an increased ATP level in mCMS-OPA1 neurons compared with CMS neurons. *D*: survival curve of mCMS-OPA1 neurons compared with non-CMS and CMS neurons after 1.5% O₂ treatment for 4 days. *E*: representative blot of caspase 3 in mCMS-OPA1 and CMS neurons after 1.5% O₂ treatment for 2 days. *F*: quantification of cleaved caspase 3 between the two groups; $n = 3$, * $P < 0.05$, ** $P < 0.01$, *** $P < 0.001$ compared with non-CMS; # $P < 0.05$, ## $P < 0.01$ compared with CMS neurons.

of CMS score across all subjects (4). In the peripheral nervous system, CMS subjects have a mild demyelination neuropathy in sural nerve biopsies (burning feet-burning hand syndromes) (41), suggesting that neuropathology of CMS might result from susceptibility to environmental stress. Over the past two decades, CMS research has shifted from physiology to genetics with the development of new technologies such as microarrays and genome sequencing. Although genetic signature of high-altitude adaptation has been demonstrated through many studies (2, 28), our understanding of CMS pathology at the cellular level is still lagging behind because of the lack of human samples and study techniques.

The availability of induced pluripotent stem cell technology can now help to overcome these limitations. Disease-specific iPSCs have been well accepted as a means for a better understanding of the basis of genetic diseases (40). As a proof of concept, our laboratory has confirmed that iPSC-derived blood

cells from CMS subjects have remarkable polycythemic response under hypoxia treatment compared with non-CMS subjects under the same conditions, which precisely mimics the CMS polycythemia in vitro (3), further proving that studies using CMS-specific iPSCs can lead us to unravel the basis of CMS pathology.

There are potentially a number of questions that could be asked about our present findings in this work, for example: 1) Are there differences between CMS and non-CMS populations that would predispose the CMS population to disease phenotype, especially in the CNS, at high altitude? 2) Although iPSC cell technology is an important advance and often helpful to study a disease phenotype without obtaining tissue from the specific organ under consideration, what is the specific rationale for our use of these cells and for the use of neurons subsequently? And 3) are the changes observed in CMS cells as a result of hypoxia, inherent properties of the cells, or other

types of stresses of high altitude? To address such questions, we should highlight the context and background of the research that we have undertaken for the past several years (2, 3, 18, 29, 32, 36, 37, 42, 48, 50, 51). In particular, we have done a large number of whole genome sequencing on high-altitude dwellers to investigate genetic differences between CMS and non-CMS (32, 51). Through these studies we have learned, for example, that non-CMS subjects have adapted to high altitude via germ line beneficial mutations that occurred over prolonged periods (e.g., thousands of years), but these specific mutations are not existent in CMS subjects, hence the maladaptation of the CMS population to high altitude and their manifestation of disease in such environments. This led us to conclude that the CMS population is genetically different and predisposed to disease phenotype. Interestingly, they manifest the disease phenotype only at high altitude. Our hypothesis that hypoxia is the major environmental stress condition that uncovers the predisposition is borne out by our already published results. For example, red blood cells (generated from CMS and non-CMS fibroblasts and subsequent iPSC cells) proliferate tremendously *in vitro* only on exposure to hypoxia in CMS cells but not in non-CMS cells (3). Hence we believe that the different genetic makeup of CMS cells predispose them to disease only during certain conditions (hypoxia seemingly being one major stress factor). Hence our rationale for the use of iPSC cells is that the genetic differences that we detected between CMS and non-CMS (by whole genome sequencing) (37) would be maintained in these iPSC cells (or their derivatives such as neurons) and would allow us to determine any differences between these two populations. The fact that hypoxia was a major factor in inducing the disease phenotype in our previous studies does not preclude other forms of stress (such as radiation exposure) on these populations, although we do not have any evidence so far for the effect of such stresses. Furthermore, that CMS subjects cease to have major symptoms after descent to low altitude should not imply that their tissues have no abnormalities, such as the ones we have shown in the present work. So far, there have been no investigations of mitochondria of CMS and non-CMS at the level of detail we have provided herein. The usefulness of acute hypoxia in our studies relates to our interest to perturb the system to better understand its vulnerability and not as much to mimic long-term hypoxia as in CMS.

Mitochondrial has been shown to play an important role in adaptation (13, 21, 29). For instance, Li et al. (21) found that mitochondrial haplogroups G and M9a1a1c1b, especially with the T 3394C (ND1) and G7697A (COXII) variants, might be the cause of hypoxic adaptation in Tibetans. In animal models, rats that were preconditioned with mild intermittent hypobaric hypoxia can adapt and protect themselves from subsequent severe hypobaric hypoxia-induced injury. This adaptation is obtained through stabilization of mitochondrial function by the PGC-1 α /ERR α /MFN2 regulatory pathway (13). Therefore we hypothesized that mitochondrial modification could be involved in hypoxia adaptation in highlanders, and the differences of mitochondrial morphology and function between CMS and non-CMS neurons may provide us with clues to better understand hypoxia adaptation and maladaptation

As highly dynamic organelles, mitochondria are constantly undergoing fission and fusion (11), and well-maintained mitochondrial homeostasis is critical for maintaining normal cellular function. Alterations in various aspects of mitochondrial

biology could disrupt mitochondrial homeostasis and result in mitochondrial dysfunction. Such dysfunction has been shown to be one of the predominant features in neurodegenerative diseases, such as Alzheimer's disease, Parkinson's disease, and amyotrophic lateral sclerosis (34).

Previous work from our laboratory has shown that hypoxia-adapted *Drosophila*, which can survive under extreme lethal hypoxic conditions (4%) for over many generations, exhibit an increased mitochondrial volume density and cristae abundance (29). In contrast, loss of mitochondrial volume density can be observed in rat hippocampal neurons after acute hypobaric hypoxia treatment (e.g., 3 and 7 days) (17), suggesting that increased mitochondrial density and cristae abundance might be beneficial and promote survival. Therefore the decreased mitochondrial volume density, and cristae abundance, observed in CMS neurons might be detrimental and lead to a predisposition to stress sensitivity.

PGC-1 α , a master regulator of mitochondrial biogenesis, has been shown to regulate mitochondrial density in all subtypes of neurons (46) and is downregulated in CMS neurons. Previous studies have shown that PGC-1 α knockout mice have a reduced number of functional mitochondria, reduced capacity of sustaining running exercise, and a lower fatigue resistance index (20, 34), leading us to speculate that certain CMS neurologic symptoms, such as mental and physical fatigue, might be due to loss of functional mitochondria in CMS neurons.

Interestingly, Bao et al. (4) reported that CMS patients experienced reduced cerebral blood flow and delayed cerebral circulation, in which the reduction of cerebral blood flow are correlated with the increasing severity of CMS score across all subjects. Global hypoxia leads to mitochondrial ultrastructural changes (9) and an imbalance in mitochondrial dynamics in rat hippocampus neurons (17). Therefore it is not surprising to find smaller mitochondria in CMS neurons. Mitochondrial size is determined by a balance between fusion and fission, and both fission genes (DRP1 and FIS1) and fusion genes (OPA1 and MFN2) were underexpressed in CMS neurons. Loss of DRP1 rapidly eliminates dopaminergic neuron terminals in midbrain and causes cell body degeneration (8), and loss of MFN2 contributes to the age-dependent progressive loss of dopaminergic neurons in the striatum (30), suggesting that loss of both fusion and fission genes could interrupt mitochondrial homeostasis and affect mitochondrial functions. Although both fission and fusion genes were downregulated in CMS neurons, the shorter mitochondrial length suggested that fission may predominate over fusion in CMS neurons.

OPA1, which is one of the most well studied mitochondrial dynamic genes, not only plays an important role in mitochondrial fusion but also in mitochondrial biogenesis, cristae remodeling, and cell death. Under physiological conditions, a similar amount of L- and S-OPA1 are formed (44), with L-OPA1 promoting fusion and S-OPA1 promoting fission, such that the relative amount of L-OPA1 and S-OPA1 determines the balance of mitochondrial fusion and fission as well as mitochondrial morphology and function (24, 35). Under pathological conditions, such as oxygen and glucose deprivation or hypoxia/ischemia, the loss of L-OPA1 and accumulation of S-OPA1 lead to the loss of cristae structures and mitochondrial fragmentation, which disturb oxidative phosphorylation, reduce ATP production, and sensitize cells to

excitotoxicity, eventually inducing apoptosis and cell death (5, 6, 10, 16, 25, 35). Indeed, we observed significantly increased S-OPA1 accumulation in CMS neurons with decreased ATP levels and increased cell death under hypoxia compared with non-CMS neurons, suggesting that CMS neurons might be under pathological conditions.

The mitochondrial-mediated intrinsic cell death pathway involves Bax and Bak, cytochrome C release, and downstream caspase 3 activation (26). Overexpression of cleaved caspase 3 in CMS neurons further confirmed caspase 3-mediated cell death in CMS neurons under hypoxic stress. Restoration of L-OPA1 can inhibit hypoxia ischemia-induced retinal injury by conserving ATP production, blunting mitochondrial dysfunction, and inhibiting cytochrome C release (7, 14, 39). Here, through manipulation of OPA1 expression and improving the balance between L-OPA1 and S-OPA1 in mCMS-OPA1 neurons, the survival rate is significantly improved compared with that in the CMS neurons after hypoxic treatment, showing that an appropriate ratio of L-OPA1 and S-OPA1 is important for maintaining normal cellular functions in CMS neurons. Previous studies have demonstrated that activation of caspase 3 can be detected as early as 2 h after hypoxia treatment and maximized at 24 or 48 h (1, 12, 47, 49). In the present study, cleaved caspase 3 in the mCMS-OPA1 neurons was significantly lower than in CMS neurons after 2 days of hypoxic treatment, illustrating that an improved balance between L- and S-OPA1 in mCMS-OPA1 can delay the early initiation of caspase 3-mediated cell death in CMS neurons and therefore improve the survival rate under hypoxia. Of particular interest is that the survival rate in mCMS-OPA neurons under hypoxia is still significantly lower than in non-CMS neurons, suggesting that mitochondrial fragmentation due to the loss of balance between L-OPA1 and S-OPA1 in CMS neurons contributes only partially to the vulnerability of the phenotype in CMS neurons. We used iPSC-derived disease-specific neurons as a model to investigate the mechanisms of neuropathology in CMS neurons. We report that CMS neurons exhibit altered mitochondrial morphology and dynamics that renders CMS neurons more vulnerable to hypoxic stress compared with non-CMS neurons. Our data are the first to provide evidence demonstrating the relationship between mitochondrial dysfunction and neuropathology in CMS subjects.

We conclude that CMS neurons have altered mitochondrial morphology and dynamics, accompanied by increased cell death under hypoxia when compared with non-CMS neurons. By manipulating the OPA1 gene, we demonstrate that altered mitochondrial dynamics is one of the reasons for the increased susceptibility of CMS neurons to stress conditions.

GRANTS

Support for this study was provided by National Institutes of Health Grants 1R21 NS-101652-01 (to G. Haddad), R01 NS-065874 (to A. La Spada), P41 GM-103412 (to M. Ellisman), and P30 NS-047101 (to the UCSD School of Medicine Microscopy Core).

DISCLOSURES

No conflicts of interest, financial or otherwise, are declared by the authors.

AUTHOR CONTRIBUTIONS

H.Z., D.C., O.A., A.R.L.S., and G.G.H. conceived and designed research; H.Z., G.P., H.Y., D.C., and O.A. performed experiments; H.Z., G.P., H.Y., and M.E. analyzed data; H.Z. and G.P. interpreted results of experiments; H.Z. and

G.P. prepared figures; H.Z., G.P., and H.Y. drafted manuscript; H.Z., G.P., H.Y., O.A., M.E., A.R.L.S., and G.G.H. edited and revised manuscript; H.Z., G.P., H.Y., D.C., O.A., M.E., A.R.L.S., and G.G.H. approved final version of manuscript.

REFERENCES

- Araya R, Uehara T, Nomura Y. Hypoxia induces apoptosis in human neuroblastoma SK-N-MC cells by caspase activation accompanying cytochrome c release from mitochondria. *FEBS Lett* 439: 168–172, 1998. doi:10.1016/S0014-5793(98)01363-5.
- Azad P, Stobdan T, Zhou D, Hartley I, Akbari A, Bafna V, Haddad GG. High-altitude adaptation in humans: from genomics to integrative physiology. *J Mol Med (Berl)* 95: 1269–1282, 2017. doi:10.1007/s00109-017-1584-7.
- Azad P, Zhao HW, Cabrales PJ, Ronen R, Zhou D, Poulsen O, Appenzeller O, Hsiao YH, Bafna V, Haddad GG. Senp1 drives hypoxia-induced polycythemia via GATA1 and Bcl-xL in subjects with Monge's disease. *J Exp Med* 213: 2729–2744, 2016. doi:10.1084/jem.20151920.
- Bao H, Wang D, Zhao X, Wu Y, Yin G, Meng L, Wang F, Ma L, Hackett P, Ge RL. Cerebral edema in chronic mountain sickness: a new finding. *Sci Rep* 7: 43224, 2017. doi:10.1038/srep43224.
- Barbour JA, Turner N. Mitochondrial stress signaling promotes cellular adaptations. *Int J Cell Biol* 2014: 156020, 2014. doi:10.1155/2014/156020.
- Baricault L, Ségué B, Guégand L, Olichon A, Valette A, Larminat F, Lenaers G. OPA1 cleavage depends on decreased mitochondrial ATP level and bivalent metals. *Exp Cell Res* 313: 3800–3808, 2007. doi:10.1016/j.yexcr.2007.08.008.
- Belleguer P, Pellegrini L. The dynamin GTPase OPA1: more than mitochondria? *Biochim Biophys Acta* 1833: 176–183, 2013. doi:10.1016/j.bbamcr.2012.08.004.
- Berthet A, Margolis EB, Zhang J, Hsieh I, Zhang J, Hnasko TS, Ahmad J, Edwards RH, Sesaki H, Huang EJ, Nakamura K. Loss of mitochondrial fission depletes axonal mitochondria in midbrain dopamine neurons. *J Neurosci* 34: 14304–14317, 2014. doi:10.1523/JNEUROSCI.0930-14.2014.
- Biswal S, Sharma D, Kumar K, Nag TC, Barhwal K, Hota SK, Kumar B. Global hypoxia induced impairment in learning and spatial memory is associated with precocious hippocampal aging. *Neurobiol Learn Mem* 133: 157–170, 2016. doi:10.1016/j.nlm.2016.05.011.
- Brooks C, Cho SG, Wang CY, Yang T, Dong Z. Fragmented mitochondria are sensitized to Bax insertion and activation during apoptosis. *Am J Physiol Cell Physiol* 300: C447–C455, 2011. doi:10.1152/ajpcell.00402.2010.
- Carelli V, Maresca A, Caporali L, Trifunov S, Zanna C, Rugolo M. Mitochondria: Biogenesis and mitophagy balance in segregation and clonal expansion of mitochondrial DNA mutations. *Int J Biochem Cell Biol* 63: 21–24, 2015. doi:10.1016/j.biocel.2015.01.023.
- Chao W, Shen Y, Li L, Rosenzweig A. Importance of FADD signaling in serum deprivation- and hypoxia-induced cardiomyocyte apoptosis. *J Biol Chem* 277: 31639–31645, 2002. doi:10.1074/jbc.M204104200.
- Chitra L, Boopathy R. Altered mitochondrial biogenesis and its fusion gene expression is involved in the high-altitude adaptation of rat lung. *Respir Physiol Neurobiol* 192: 74–84, 2014. doi:10.1016/j.resp.2013.12.007.
- Civiletto G, Varanita T, Cerutti R, Gorletta T, Barbaro S, Marchet S, Lamperti C, Viscomi C, Scorrano L, Zeviani M. Opa1 overexpression ameliorates the phenotype of two mitochondrial disease mouse models. *Cell Metab* 21: 845–854, 2015. doi:10.1016/j.cmet.2015.04.016.
- DiMauro S, Schon EA. Mitochondrial disorders in the nervous system. *Annu Rev Neurosci* 31: 91–123, 2008. doi:10.1146/annurev.neuro.30.051606.094302.
- Duvezin-Caubet S, Jagasia R, Wagener J, Hofmann S, Trifunovic A, Hansson A, Chomyn A, Bauer MF, Attardi G, Larsson NG, Neupert W, Reichert AS. Proteolytic processing of OPA1 links mitochondrial dysfunction to alterations in mitochondrial morphology. *J Biol Chem* 281: 37972–37979, 2006. doi:10.1074/jbc.M606059200.
- Jain K, Prasad D, Singh SB, Kohli E. Hypobaric hypoxia imbalances mitochondrial dynamics in rat brain hippocampus. *Neurol Res Int* 2015: 742059, 2015. doi:10.1155/2015/742059.
- Jha AR, Zhou D, Brown CD, Kreitman M, Haddad GG, White KP. Shared genetic signals of hypoxia adaptation in drosophila and in high-altitude human populations. *Mol Biol Evol* 33: 501–517, 2016. doi:10.1093/molbev/msv248.

19. **Khurana P, Ashraf QM, Mishra OP, Delivoria-Papadopoulos M.** Effect of hypoxia on caspase-3, -8, and -9 activity and expression in the cerebral cortex of newborn piglets. *Neurochem Res* 27: 931–938, 2002. doi:10.1023/A:1020347732741.
20. **Leone TC, Lehman JJ, Finck BN, Schaeffer PJ, Wende AR, Boudina S, Courtois M, Wozniak DF, Sambandam N, Bernal-Mizrachi C, Chen Z, Holloszy JO, Medeiros DM, Schmidt RE, Saffitz JE, Abel ED, Semenkovich CF, Kelly DP.** PGC-1 α deficiency causes multi-system energy metabolic derangements: muscle dysfunction, abnormal weight control and hepatic steatosis. *PLoS Biol* 3: e101, 2005. doi:10.1371/journal.pbio.0030101.
21. **Li Q, Lin K, Sun H, Liu S, Huang K, Huang X, Chu J, Yang Z.** Mitochondrial haplogroup M9a1a1c1b is associated with hypoxic adaptation in the Tibetans. *J Hum Genet* 61: 1021–1026, 2016. doi:10.1038/jhg.2016.95.
22. **Liesa M, Palacín M, Zorzano A.** Mitochondrial dynamics in mammalian health and disease. *Physiol Rev* 89: 799–845, 2009. doi:10.1152/physrev.00030.2008.
23. **Lin MT, Beal MF.** Mitochondrial dysfunction and oxidative stress in neurodegenerative diseases. *Nature* 443: 787–795, 2006. doi:10.1038/nature05292.
24. **MacVicar T, Langer T.** OPA1 processing in cell death and disease—the long and short of it. *J Cell Sci* 129: 2297–2306, 2016. doi:10.1242/jcs.159186.
25. **Merkwirth C, Dargazanli S, Tatsuta T, Geimer S, Löwer B, Wunderlich FT, von Kleist-Retzow JC, Waisman A, Westermann B, Langer T.** Prohibitins control cell proliferation and apoptosis by regulating OPA1-dependent cristae morphogenesis in mitochondria. *Genes Dev* 22: 476–488, 2008. doi:10.1101/gad.460708.
26. **Ow YP, Green DR, Hao Z, Mak TW.** Cytochrome *c*: functions beyond respiration. *Nat Rev Mol Cell Biol* 9: 532–542, 2008. doi:10.1038/nrm2434.
27. **Penaloza D, Arias-Stella J.** The heart and pulmonary circulation at high altitudes: healthy highlanders and chronic mountain sickness. *Circulation* 115: 1132–1146, 2007. doi:10.1161/CIRCULATIONAHA.106.624544.
28. **Peng Y, Cui C, He Y, Ouzhuluobu, Zhang H, Yang D, Zhang Q, Bianbazhuoma, Yang L, He Y, Xiang K, Zhang X, Bhandari S, Shi P, Yangla, Dejiquzong, Baimakangzhuo, Duoqizhuoma, Pan Y, Cirenyangji, Baimayangji, Gonggalanzi, Bai C, Bianba, Basang, Ciwang-sangbu, Xu S, Chen H, Liu S, Wu T, Qi X, Su B.** Down-regulation of EPAS1 transcription and genetic adaptation of Tibetans to high-altitude hypoxia. *Mol Biol Evol* 34: 818–830, 2017. doi:10.1093/molbev/msw280.
29. **Perkins G, Hsiao YH, Yin S, Tjong J, Tran MT, Lau J, Xue J, Liu S, Ellisman MH, Zhou D.** Ultrastructural modifications in the mitochondria of hypoxia-adapted *Drosophila melanogaster*. *PLoS One* 7: e45344, 2012. doi:10.1371/journal.pone.0045344.
30. **Pham AH, Meng S, Chu QN, Chan DC.** Loss of Mfn2 results in progressive, retrograde degeneration of dopaminergic neurons in the nigrostriatal circuit. *Hum Mol Genet* 21: 4817–4826, 2012. doi:10.1093/hmg/dds311.
31. **Reddy PH.** Role of mitochondria in neurodegenerative diseases: mitochondria as a therapeutic target in Alzheimer's disease. *CNS Spectr* 14, Suppl 7: 8–13, 2009. doi:10.1017/S1092852900024901.
32. **Ronen R, Zhou D, Bafna V, Haddad GG.** The genetic basis of chronic mountain sickness. *Physiology (Bethesda)* 29: 403–412, 2014. doi:10.1152/physiol.00008.2014.
33. **Sanderson TH, Raghunayakula S, Kumar R.** Release of mitochondrial Opa1 following oxidative stress in HT22 cells. *Mol Cell Neurosci* 64: 116–122, 2015. doi:10.1016/j.mcn.2014.12.007.
34. **Sheng B, Wang X, Su B, Lee HG, Casadesu G, Perry G, Zhu X.** Impaired mitochondrial biogenesis contributes to mitochondrial dysfunction in Alzheimer's disease. *J Neurochem* 120: 419–429, 2012. doi:10.1111/j.1471-4159.2011.07581.x.
35. **Song Z, Chen H, Fiket M, Alexander C, Chan DC.** OPA1 processing controls mitochondrial fusion and is regulated by mRNA splicing, membrane potential, and Yme1L. *J Cell Biol* 178: 749–755, 2007. doi:10.1083/jcb.200704110.
36. **Stobdan T, Akbari A, Azad P, Zhou D, Poulsen O, Appenzeller O, Gonzales GF, Telenti A, Wong EHM, Saini S, Kirkness EF, Venter JC, Bafna V, Haddad GG.** New insights into the genetic basis of Monge's disease and adaptation to high-altitude. *Mol Biol Evol* 34: 3154–3168, 2017. doi:10.1093/molbev/msx239.
37. **Stobdan T, Zhou D, Ao-Ieong E, Ortiz D, Ronen R, Hartley I, Gan Z, McCulloch AD, Bafna V, Cabrales P, Haddad GG.** Endothelin receptor B, a candidate gene from human studies at high altitude, improves cardiac tolerance to hypoxia in genetically engineered heterozygote mice. *Proc Natl Acad Sci USA* 112: 10425–10430, 2015. doi:10.1073/pnas.1507486112.
38. **Su B, Wang X, Zheng L, Perry G, Smith MA, Zhu X.** Abnormal mitochondrial dynamics and neurodegenerative diseases. *Biochim Biophys Acta* 1802: 135–142, 2010. doi:10.1016/j.bbadis.2009.09.013.
39. **Sun Y, Xue W, Song Z, Huang K, Zheng L.** Restoration of Opa1-long isoform inhibits retinal injury-induced neurodegeneration. *J Mol Med (Berl)* 94: 335–346, 2016. doi:10.1007/s00109-015-1359-y.
40. **Tang S, Xie M, Cao N, Ding S.** Patient-specific induced pluripotent stem cells for disease modeling and phenotypic drug discovery. *J Med Chem* 59: 2–15, 2016. doi:10.1021/acs.jmedchem.5b00789.
41. **Thomas PK, King RH, Feng SF, Muddle JR, Workman JM, Gamboa J, Tapia R, Vargas M, Appenzeller O.** Neurological manifestations in chronic mountain sickness: the burning feet-burning hands syndrome. *J Neurol Neurosurg Psychiatry* 69: 447–452, 2000. doi:10.1136/jnnp.69.4.447.
42. **Udpa N, Ronen R, Zhou D, Liang J, Stobdan T, Appenzeller O, Yin Y, Du Y, Guo L, Cao R, Wang Y, Jin X, Huang C, Jia W, Cao D, Guo G, Claydon VE, Hainsworth R, Gamboa JL, Zibenigus M, Zenebe G, Xue J, Liu S, Frazer KA, Li Y, Bafna V, Haddad GG.** Whole genome sequencing of Ethiopian highlanders reveals conserved hypoxia tolerance genes. *Genome Biol* 15: R36, 2014. doi:10.1186/gb-2014-15-2-r36.
43. **Villafuerte FC, Corante N.** Chronic mountain sickness: clinical aspects, etiology, management, and treatment. *High Alt Med Biol* 17: 61–69, 2016. doi:10.1089/ham.2016.0031.
44. **Wai T, Langer T.** Mitochondrial dynamics and metabolic regulation. *Trends Endocrinol Metab* 27: 105–117, 2016. doi:10.1016/j.tem.2015.12.001.
45. **Wang X, Su B, Lee HG, Li X, Perry G, Smith MA, Zhu X.** Impaired balance of mitochondrial fission and fusion in Alzheimer's disease. *J Neurosci* 29: 9090–9103, 2009. doi:10.1523/JNEUROSCI.1357-09.2009.
46. **Wareski P, Vaarmann A, Choubey V, Safiulina D, Liiv J, Kuum M, Kaasik A.** PGC-1 α and PGC-1 β regulate mitochondrial density in neurons. *J Biol Chem* 284: 21379–21385, 2009. doi:10.1074/jbc.M109.018911.
47. **Yoshimura S, Banno Y, Nakashima S, Takenaka K, Sakai H, Nishimura Y, Sakai N, Shimizu S, Eguchi Y, Tsujimoto Y, Nozawa Y.** Ceramide formation leads to caspase-3 activation during hypoxic PC12 cell death. Inhibitory effects of Bcl-2 on ceramide formation and caspase-3 activation. *J Biol Chem* 273: 6921–6927, 1998. doi:10.1074/jbc.273.12.6921.
48. **Zhao HW, Gu XQ, Chailangkarn T, Perkins G, Callacondo D, Appenzeller O, Poulsen O, Zhou D, Muotri AR, Haddad GG.** Altered iPSC-derived neurons' sodium channel properties in subjects with Monge's disease. *Neuroscience* 288: 187–199, 2015. doi:10.1016/j.neuroscience.2014.12.039.
49. **Zheng X, Zheng X, Wang X, Ma Z, Gupta Sunkari V, Botusan I, Takeda T, Björklund A, Inoue M, Catrina SB, Brismar K, Poellinger L, Pereira TS.** Acute hypoxia induces apoptosis of pancreatic β -cell by activation of the unfolded protein response and upregulation of CHOP. *Cell Death Dis* 3: e322, 2012. doi:10.1038/cddis.2012.66.
50. **Zhou D, Haddad GG.** Genetic analysis of hypoxia tolerance and susceptibility in *Drosophila* and humans. *Annu Rev Genomics Hum Genet* 14: 25–43, 2013. doi:10.1146/annurev-genom-091212-153439.
51. **Zhou D, Udpa N, Ronen R, Stobdan T, Liang J, Appenzeller O, Zhao HW, Yin Y, Du Y, Guo L, Cao R, Wang Y, Jin X, Huang C, Jia W, Cao D, Guo G, Gamboa JL, Villafuerte F, Callacondo D, Xue J, Liu S, Frazer KA, Li Y, Bafna V, Haddad GG.** Whole-genome sequencing uncovers the genetic basis of chronic mountain sickness in Andean highlanders. *Am J Hum Genet* 93: 452–462, 2013. doi:10.1016/j.ajhg.2013.07.011.